

Polarization Effects in Two-Photon Free-Free Transitions in Laser-Assisted Electron-Hydrogen Collisions

Aurelia Cionga and Gabriela Buica

*Institute for Space Sciences, P.O. Box MG-36,
Bucharest-Măgurele, Bucharest, R-76900 Romania*

Abstract

Two-photon free-free transitions in elastic laser-assisted electron-hydrogen collisions are studied in the domain of high scattering energies and low or moderate field intensities, in the third order of perturbation theory, taking into account all the involved Feynman diagrams. Based on the analytical expressions of the transition amplitudes, the differential cross sections for two-photon absorption/emission are computed at impact energy $E_i = 100$ eV. The effect of field polarizations on the angular distribution and on the frequency dependence of the differential cross section is analyzed.

Keywords:

I. INTRODUCTION

Recently, a series of experimental [1] and theoretical [2] works have been devoted to the study of free-free transitions in laser-assisted elastic electron-atom collisions at low scattering energies.

It is the aim of this work to investigate free-free transitions in a different regime, that of high scattering energies and low or moderate field intensities such that the use of perturbation theory might provide a sensible description of the process. We focus our attention on the study of free-free transitions that involve the absorption/emission of two *different* photons by the compound projectile-target system in an external radiation field. The target is the hydrogen atom in the ground state. The process can be formally represented by

$$H(E_{1s}) + e^- (\vec{k}_i, E_i) \pm [\gamma(\vec{\epsilon}_1, \omega_1) + \gamma(\vec{\epsilon}_2, \omega_2)] \rightarrow H(E_{1s}) + e^- (\vec{k}_f, E_f), \quad (1)$$

where $E_{i(f)}$, $\vec{k}_{i(f)}$ are the initial (final) energy and momentum of the projectile; ω_j , $\vec{\epsilon}_j$ denote the frequency and the polarization vector of the photon j ($j = 1, 2$). The upper sign corresponds to the absorption of both photons, the lower one corresponds to their stimulated emission.

The process (1) has been previously investigated for two *identical* photons. Kracke *et al* [3] have studied the differential cross section of two-photon free-free transitions at high scattering energies (50-500 eV) for photon energies below the ionization threshold of hydrogen ($\omega < 20$ eV). They have used in their work the lowest order perturbation theory, taken into account all the involved Feynman diagrams. For strong fields, the laser-particle interaction must be treated beyond the perturbation theory. In this context, Dörr *et al* [4] developed the Born-Floquet theory, in which both laser-projectile and laser-target interactions are treated exactly. This approach is valid in the domain of high scattering energies since it involves the first Born approximation to treat the projectile-target interaction. We refer to this paper for a comprehensive analysis of other previous works.

In Sec. II we present the formalism we have used to evaluate transition matrix elements for two-photon absorption/emission: the projectile-target interaction as well as the interaction between the electrons and the electromagnetic field have been treated perturbatively. We have evaluated the analytic expressions of the corresponding transition amplitudes in the third order of perturbation theory, including the twenty-four Feynman diagrams. The third

section is devoted to the discussion of the numerical results. We report here our results concerning the influence of the state of polarization of the two photons on the differential cross section of the scattered electron. We claim that this effect is significant in the domain in which the dressing of the target is important: at small scattering angles in general and in particular close to atomic resonances.

II. BASIC EQUATIONS

The time evolution of the electron-hydrogen system in the presence of an electromagnetic field described by the vector potential

$$\vec{\mathcal{A}}(t) = \vec{\varepsilon}_1 A_{01} \cos(\omega_1 t) + \vec{\varepsilon}_2 A_{02} \cos(\omega_2 t), \quad (2)$$

is governed by the hamiltonian

$$\begin{aligned} \mathcal{H} &= \frac{\vec{p}^2}{2} - \frac{1}{r} + \frac{\vec{P}^2}{2} + \frac{1}{|\vec{r} - \vec{R}|} - \frac{1}{R} + \frac{1}{c} [\vec{p} + \vec{P}] \cdot \vec{\mathcal{A}}(t) \\ &\equiv H_0 + V + W(t), \end{aligned} \quad (3)$$

where \vec{r} , \vec{p} are the position and momentum operator of the bound (atomic) electron and \vec{R} , \vec{P} are the position and momentum operator of the free (projectile) electron. $V \equiv -R^{-1} + |\vec{r} - \vec{R}|^{-1}$ denotes the e-H interaction in the direct channel and $W(t) \equiv c^{-1} [\vec{p} + \vec{P}] \cdot \vec{\mathcal{A}}(t)$ denotes the interaction of the charge particles with the field, treated in the velocity gauge, using the dipole approximation. The $\vec{\mathcal{A}}^2$ -term was eliminated through a unitary transformation.

In the *first nonvanishing order* of the perturbation theory, the S -matrix elements corresponding to two-photon processes are given by

$$S^{(2)} = - \int_{-\infty}^{+\infty} dt_1 \int_{-\infty}^{t_1} dt_2 < \chi_f^- | \tilde{W}(t_1) \tilde{W}(t_2) | \chi_i^+ >, \quad (4)$$

where $\tilde{W}(t) = e^{iH_0 t} W(t) e^{-iH_0 t}$. In the previous equation $|\chi_i^+ >$ and $|\chi_f^- >$ describe the initial and final states of the colliding system (electron-atom)

$$|\chi_i^+ > = |\Psi_i > + G^+(\mathcal{E}_i) V |\Psi_i >, \quad (5)$$

$$|\chi_f^- > = |\Psi_f > + G^-(\mathcal{E}_f) V |\Psi_f >, \quad (6)$$

where

$$G^\pm(\mathcal{E}) = [\mathcal{E} - H_0 - V \pm i\delta]^{-1} \quad (7)$$

and δ a positive infinitesimal number. $|\Psi_{i,f}\rangle$ are the asymptotic states corresponding to the colliding system in the absence of the interaction V

$$|\Psi_i\rangle = |\psi_{1s}\rangle |K_i\rangle, \quad (8)$$

$$|\Psi_f\rangle = |\psi_{1s}\rangle |K_f\rangle. \quad (9)$$

Here $|\psi_{1s}\rangle$ denotes the ground state of a hydrogen atom and $|K_{i,f}\rangle$ are plane waves. The initial and final energies of the electron-atom system are

$$\mathcal{E}_i = E_{1s} + \frac{k_i^2}{2}, \quad (10)$$

$$\mathcal{E}_f = E_{1s} + \frac{k_f^2}{2} \pm (\omega_1 + \omega_2). \quad (11)$$

The transition-matrix element involving two *different* photons, both absorbed or emitted, is given by

$$T^{(2)} = \frac{1}{4}(1 + \mathcal{P}_{12})\chi_f^- |\vec{A}_1 \cdot (\vec{p} + \vec{P}) G^+(\mathcal{E}_i \pm \omega_2) \vec{A}_2 \cdot (\vec{p} + \vec{P})| \chi_i^+ \rangle, \quad (12)$$

where \mathcal{P}_{12} is the permutation operator between the vector potentials $\vec{A}_j = \vec{\varepsilon}_j A_{0j}$ ($j=1,2$), which describe the two components of the field (2). In Eq.(12) the upper sign corresponds to absorption, the lower one to stimulated emission. It is possible to write this matrix element as the sum of three terms, each of them connected with specific Feynman diagrams, as we shall discuss later in this section. These terms are:

- *the electronic term*

$$T_P = \frac{1}{4}(1 + \mathcal{P}_{12}) \langle \chi_f^- | \vec{A}_1 \cdot \vec{P} G^+(\mathcal{E}_i \pm \omega_2) \vec{A}_2 \cdot \vec{P} | \chi_i^+ \rangle, \quad (13)$$

- *the mixed term*

$$T_M = \frac{1}{4}(1 + \mathcal{P}_{12})(1 + \mathcal{P}_{\vec{p}\vec{P}}) \langle \chi_f^- | \vec{A}_1 \cdot \vec{p} G^+(\mathcal{E}_i \pm \omega_2) \vec{A}_2 \cdot \vec{P} | \chi_i^+ \rangle, \quad (14)$$

where $\mathcal{P}_{\vec{p}\vec{P}}$ is the permutation operator between \vec{p} and \vec{P} , and

- *the atomic term*

$$T_A = \frac{1}{4}(1 + \mathcal{P}_{12}) \langle \chi_f^- | \vec{A}_1 \cdot \vec{p} G^+(\mathcal{E}_i \pm \omega_2) \vec{A}_2 \cdot \vec{p} | \chi_i^+ \rangle. \quad (15)$$

Since we restrict ourselves to the domain of high scattering energies, we use the first Born approximation to treat electron-atom scattering, which implies

$$|\chi_i^+\rangle \simeq |\Psi_i\rangle + G_0^+(\mathcal{E}_i)V|\Psi_i\rangle, \quad (16)$$

$$|\chi_f^-\rangle \simeq |\Psi_f\rangle + G_0^-(\mathcal{E}_f)V|\Psi_f\rangle, \quad (17)$$

where

$$G_0^\pm(\mathcal{E}) = [\mathcal{E} - H_0 \pm i\delta]^{-1}. \quad (18)$$

In this way, the evaluation of the transition matrix element is made in the third order of perturbation theory: the second order in the electric field and the first order in the scattering potential, V .

A. Electronic term

The electronic term is connected to six Feynman diagrams in which only the projectile exchanges two different photons with the field (2). Only three of these diagrams are represented in Fig.1(a), the other three are obtained by interchanging ω_1 and ω_2 .

In the standard way, after integration over the projectile coordinates, the electronic term in Eq.(13) may be written as

$$T_P = \frac{\sqrt{I_1 I_2}}{4\omega_1^2 \omega_2^2} (\vec{\varepsilon}_1 \cdot \vec{q})(\vec{\varepsilon}_2 \cdot \vec{q}) < \psi_{1s} | F(\vec{q}) | \psi_{1s} >, \quad (19)$$

where I_j is the intensity of the component j of the field (2), \vec{q} is the momentum transfer of the projectile and $F(\vec{q})$ is the form factor operator

$$F(\vec{q}) = \frac{1}{2\pi^2 q^2} [\exp(i\vec{q} \cdot \vec{r}) - 1].$$

We remind that this is the only term which gives contributions to the weak field intensity limit of Bunkin-Fedorov formula [5]. That approach describes the target by a potential and neglects the atomic dressing. In order to take into account the atomic dressing we include in our calculation the other eighteen Feynman diagrams, corresponding to the mixed and atomic terms.

B. Mixed term

The mixed term is connected to twelve Feynman diagrams, in which each electron (free and bound) absorbs/emits one photon from each component of the field (2). Only six diagrams are represented in Fig.1(b), the other six are obtained again by interchanging ω_1 and ω_2 .

In order to evaluate the mixed term we took advantage of the analytic form of the vectors

$$|\vec{w}_{100}(\Omega) > = -G_C(\Omega)\vec{p}|\psi_{1s} >,$$

which were previously studied in Ref.[6]. Here $G_C(\Omega)$ is the Coulomb Green function. After integration over the projectile coordinates, the mixed term in Eq.(14) is written as

$$T_M = \mp \frac{\sqrt{I_1 I_2}}{4\omega_1 \omega_2} \left\{ \frac{\vec{\varepsilon}_2 \cdot \vec{q}}{\omega_2} \left[< \psi_{1s} | F(\vec{q}) | \vec{\varepsilon}_1 \cdot \vec{w}_{100}(\Omega_1^\pm) > < \vec{\varepsilon}_1 \cdot \vec{w}_{100}(\Omega_1^\mp) | F(\vec{q}) | \psi_{1s} > \right] \right. \\ \left. + \frac{\vec{\varepsilon}_1 \cdot \vec{q}}{\omega_1} \left[< \psi_{1s} | F(\vec{q}) | \vec{\varepsilon}_2 \cdot \vec{w}_{100}(\Omega_2^\pm) > < \vec{\varepsilon}_2 \cdot \vec{w}_{100}(\Omega_2^\mp) | F(\vec{q}) | \psi_{1s} > \right] \right\}, \quad (20)$$

where the parameters $\Omega_{1,2}^\pm$ are given by

$$\Omega_{1,2}^\pm = E_{1s} \pm \omega_{1,2}.$$

In Eq.(20) the upper signs correspond to absorption and the lower ones correspond to stimulated emission of both photons.

The atomic matrix elements in Eq.(20), which appear also in one photon processes, have been evaluated analytically [7]. Based on this result it is possible to write down the general structure of the mixed term as

$$T_M = \sqrt{I_1 I_2} (\vec{\varepsilon}_1 \cdot \vec{q}) (\vec{\varepsilon}_2 \cdot \vec{q}) \mathcal{T}_M(\omega_1, \omega_2; q), \quad (21)$$

where the radial part, $\mathcal{T}_M(\omega_1, \omega_2; q)$, is expressed in terms of hypergeometric functions.

C. Atomic term

The atomic term is connected to six Feynman diagrams in which two different photons are exchanged between the bound electron and the field (2). Only three diagrams are represented in Fig.1(c), the other three are obtained by interchanging ω_1 and ω_2 .

Our analytic formula for the atomic term is computed using the tensors

$$|w_{ij,100}(\Omega', \Omega) > = G_C(\Omega') p_i G_C(\Omega) p_j |\psi_{1s} >,$$

studied in Ref.[8]. After integration over the coordinates of the projectile, the atomic term in Eq.(15) is written as

$$T_A = \frac{\sqrt{I_1 I_2}}{4\omega_1 \omega_2} \sum_{j,l=1}^3 \varepsilon_{1j} \varepsilon_{2l} \left[< w_{j,100}(\Omega_1^\mp) | F(\vec{q}) | w_{l,100}(\Omega_2^\pm) > < w_{l,100}(\Omega_2^\mp) | F(\vec{q}) | w_{j,100}(\Omega_1^\pm) > \right]$$

$$\begin{aligned}
& + < \psi_{1s} | F(\vec{q}) | w_{jl,100}(\Omega'^{\pm}, \Omega_2^{\pm}) > < \psi_{1s} | F(\vec{q}) | w_{lj,100}(\Omega'^{\pm}, \Omega_1^{\pm}) > \\
& + < w_{lj,100}(\Omega'^{\mp}, \Omega_1^{\mp}) | F(\vec{q}) | \psi_{1s} > < w_{jl,100}(\Omega'^{\mp}, \Omega_2^{\mp}) | F(\vec{q}) | \psi_{1s} > \Big].
\end{aligned} \tag{22}$$

Here the parameter Ω' takes the values

$$\Omega^{\pm} = E_{1s} \pm (\omega_1 + \omega_2)$$

and $\Omega_{1,2}^{\pm}$ were defined above. In Eq.(22) the upper signs correspond to absorption and the lower ones correspond to emission of two different photons.

We have evaluated analytically the atomic matrix element in Eq.(22); based on this results one can write the general structure of the atomic term as

$$T_A = \sqrt{I_1 I_2} [(\vec{\varepsilon}_1 \cdot \vec{q})(\vec{\varepsilon}_2 \cdot \vec{q}) \mathcal{T}'_{\mathcal{A}}(\omega_1, \omega_2; q)(\vec{\varepsilon}_1 \cdot \vec{\varepsilon}_2) \mathcal{T}''_{\mathcal{A}}(\omega_1, \omega_2; q)], \tag{23}$$

where the radial parts, $\mathcal{T}'_{\mathcal{A}}(\omega_1, \omega_2; q)$ and $\mathcal{T}''_{\mathcal{A}}(\omega_1, \omega_2; q)$, are expressed as series of hypergeometric functions [9].

For the sake of simplicity, the equations (19-23) have been written using linear polarizations. We point out that for photon emission, one must take the complex conjugate of the polarization vector.

Finally, the differential cross section for the absorption/emission of two different photons in laser-assisted elastic electron-hydrogen collisions can be written as

$$\frac{d\sigma}{d\Omega} = (2\pi)^4 \frac{k_f}{k_i} |T_P + T_M + T_A|^2, \tag{24}$$

where the electronic, mixed, and atomic terms have the structure given in Eqs.(19, 21, 23).

III. RESULTS

We have computed the differential cross section for two-photon free-free transitions in laser-assisted elastic electron-hydrogen collisions at scattering energy $E_i = 100$ eV. We have chosen to report here the case of two laser sources having the same frequency, $\omega_1 = \omega_2 \equiv \omega$, but different polarizations. The investigated photon energies are smaller than the ionization energy of hydrogen. The results are valid for low and moderate field intensities, below 10^{10} W/cm². In all the cases that we have studied the initial momentum of the projectile, \vec{k}_i , defines the Oz -axis.

We discuss here the effect of the state of polarization of the photons on the frequency dependence of the differential cross section and on the azimuthal angular distribution of the scattered electrons, for scattering angles in the domain where target dressing effects are important. In general, this domain corresponds to small scattering angles, as it has been pointed out by Kracke *et al* [3], who studied the monochromatic case.

A. Frequency dependence

In Fig.2 we present the differential cross section for two-photon absorption in Eq.(24), normalized with respect to the field intensities, $I_1 I_2$, as a function of the photon frequency, in the range $0 < \omega < 6.8$ eV. The scattering angle, $\theta = 5^\circ$, is in the domain where the dressing effects are important. Our calculations were performed for linear polarizations. We have chosen $\vec{\varepsilon}_1 || Oz$ and $\vec{\varepsilon}_2 \perp \vec{\varepsilon}_1$, the polarization vectors defining the scattering plane.

The differential cross section (solid line) exhibits a series of resonances, located between 6 and 6.8 eV. These resonances occur at photon frequencies such that $2\omega = |E_{1s}|(1 - 1/n^2)$ for $n > 2$, where n is the principal quantum number. They correspond to poles in the radial integrals \mathcal{T}'_A and \mathcal{T}''_A , which appear in the atomic term. The resonance corresponding to $n=2$, i.e., $\omega = 5$ eV, does not exist for orthogonal polarization: the connected pole appears in Eq.(23) only in the radial integral \mathcal{T}''_A , which multiplies the scalar product $\vec{\varepsilon}_1 \cdot \vec{\varepsilon}_2$, which vanishes. To emphasize the origin of these resonances we have plotted also in Fig.2 the electronic (dotted) and mixed (dot-dashed) contributions, which were calculated when only T_P and T_M , respectively, were taken into account in Eq.(24).

We believe that this series of resonances is particularly interesting from the experimental point of view. Indeed, two-photon processes may be easier to detect at photon energies close to one of these resonances because they do not correspond to resonances of the lower order processes, namely one-photon absorption/emission.

A second series of resonances, not shown in Fig.2, is located between 10 and 13.6 eV. They occur for photon frequencies such that $\omega = |E_{1s}|(1 - 1/n^2)$, where $n \geq 2$. This time the resonances correspond to poles which exist in three radial integrals: \mathcal{T}_M , \mathcal{T}'_A , and \mathcal{T}''_A .

In Fig.2 the differential cross section (solid line) has also a series of minima. The first minimum is due to the fact that, in this geometry, the differential cross section in Eq.(24) is proportional to $|(\vec{\varepsilon}_1 \cdot \vec{q})|^2 = |k_i - k_f \cos \theta|^2$, which is vanishing at $\theta = 5^\circ$. The other minima

are due to interferences between the electronic, mixed, and atomic terms.

B. Azimuthal angular distribution

We have found out that the azimuthal angular distributions of the scattered electrons are significantly modified in the case of complex polarization vectors if virtual transitions to continuum are energetically allowed, i.e., $2\omega > |E_{1s}|$. To illustrate this remark we discuss two distinct cases. In the first case the photon frequency corresponds to KrF laser, $\omega = 5$ eV. One has $2\omega < |E_{1s}|$ and the radial integrals \mathcal{T}_M , \mathcal{T}'_A , and \mathcal{T}''_A are real. On the contrary, in the second case, when the frequency of the photons corresponds to the second harmonic of KrF, one has $2\omega > |E_{1s}|$ and the corresponding radial integrals are complex. Each of these frequencies corresponds to atomic resonances. For each of these frequencies, we present the differential cross section of two-photon absorption at a fixed scattering angle, $\theta = 20^\circ$, as a function of the azimuthal angle ϕ . Two different choices of the polarization vectors were investigated.

1. $\vec{\varepsilon}_1 = \vec{e}_z$ and $\vec{\varepsilon}_2 = (\vec{e}_z + i\vec{e}_x) / \sqrt{2}$

In this case one laser beam, which direction defines the Ox axis, is linearly polarized with the polarization vector parallel to the initial momentum of the projectile, $\vec{\varepsilon}_1 || Oz$. The other laser beam, of the same frequency, defines the Oy -axis and is circularly polarized, $\vec{\varepsilon}_2 \equiv (\vec{e}_z + i\vec{e}_x) / \sqrt{2}$.

For this choice of polarizations the electronic and the mixed terms in Eqs.(19,21) have the same ϕ -dependence, namely of the form $\alpha(\alpha + i\beta \cos \phi)$. As a consequence, the electronic and the mixed contribution to the differential cross section are symmetric with respect to the reflection in the planes xOz and yOz for both frequencies, $\omega = 5$ eV in Fig.3 and $\omega = 10$ eV in Fig.4.

The atomic term (23) has a different ϕ -dependence, given by

$$T_A \sim \mathcal{T}''_A + \alpha^2 \mathcal{T}'_A + i\alpha\beta \mathcal{T}'_A \cos \phi. \quad (25)$$

The atomic contribution has the above mentioned reflection properties only in Fig.3, where $\omega = 5$ eV. In Fig.4, where $\omega = 10$ eV, the atomic contribution has only one symmetry plane. Indeed, $\phi \rightarrow -\phi$ is a symmetry operation for the quantity in Eq.(25), therefore

xOz is a symmetry plane. yOz is no more a symmetry plane because both \mathcal{T}'_A and \mathcal{T}''_A are complex and the modulus square of the quantity in Eq.(25) is not symmetric to the change $\phi = \pi/2 - \xi \rightarrow \pi/2 + \xi$.

At small scattering angles in general and in particular close to resonances, where the dressing effects are important, there are interferences between the atomic and the mixed contributions. They impose the ϕ -dependence of the differential cross section (24), given by

$$\frac{d\sigma}{d\Omega} \sim |\mathcal{T}''_A + \alpha^2 \mathcal{T}_1 + i\alpha\beta \mathcal{T}_1 \cos \phi|^2, \quad (26)$$

where $\mathcal{T}_1 = \mathcal{T}_P + \mathcal{T}_M + \mathcal{T}'_A$ and \mathcal{T}_P is the radial part of the electronic term (19). In particular, only \mathcal{T}''_A has a pole when $\omega = 5$ eV, therefore the atomic contribution in Fig.3 is almost ϕ -independent (a circle) and it is dominant in the differential cross section. The situation is different in Fig.4 because three radial integrals, \mathcal{T}_M , \mathcal{T}'_A , and \mathcal{T}''_A , have poles when $\omega = 10$ eV.

At large scattering angles the electronic term is dominant and it imposes the angular distribution of the differential cross section.

We note also that the change from right to left circular polarization implies a simultaneous change of the sign of the last term in Eqs.(25-26), which is equivalent to a rotation by π of the curves in Figs.3-4. This rotation is visible in the angular distributions only if the radial integrals have complex values, i.e., when $2\omega > |E_{1s}|$.

$$2. \quad \vec{\varepsilon}_1 = (\vec{e}_z + i\vec{e}_x) / \sqrt{2} \text{ and } \vec{\varepsilon}_2 = (\vec{e}_y + i\vec{e}_z) / \sqrt{2}$$

In this second case both polarization vectors are right circularly polarized. The direction of the first laser beam defines the Oy -axis, the other one the Ox -axis.

The electronic and the mixed terms have again the same ϕ -dependence, given by

$$\alpha\beta(\sin \phi - \cos \phi) + i(\alpha^2 + \beta^2 \sin \phi \cos \phi).$$

For both frequencies, $\omega = 5$ eV in Fig.5 and $\omega = 10$ eV in Fig.6, the first ($\phi = \pi/4$) and the second ($\phi = 3\pi/4$) bisector of the angle xOy are symmetry axes of the electronic and the mixed contributions to the differential cross section.

The atomic term (23) has a different ϕ -dependence, namely

$$\begin{aligned} T_A \sim & \alpha\beta\mathcal{T}'_A(\sin \phi - \cos \phi) \\ & + i\left(\mathcal{T}''_A + \alpha^2\mathcal{T}'_A + \beta^2\mathcal{T}'_A \sin \phi \cos \phi\right). \end{aligned} \quad (27)$$

The atomic contribution has the two previous symmetry axes only when $\omega = 5$ eV (Fig.5); when $\omega = 10$ eV the atomic part has only one symmetry axis: along the second bisector (Fig.6). Since the atomic term is always important for the chosen value of θ , it will determine the symmetry properties of the differential cross section.

The study of two photon with left circular polarizations implies the change of the general sign in the second line of Eq.(27). The corresponding curves are rotated by π around the Oz -axis. Due to the number of symmetry axis, this rotation is relevant only for the atomic contribution and the differential cross section in Fig.6, where $2\omega > |E_{1s}|$.

IV. CONCLUSIONS

Our investigations show that the differential cross sections for two-photon free-free transitions is strongly influenced by the state of polarization of the two photons in the domain where the dressing effects are important, that means for small scattering angles and in the vicinity of atomic resonances.

When at least one polarization vector is complex, one mirror symmetry is broken in the azimuthal angular distribution of the scattered electron if the virtual transitions to continuum of the bound electron are energetically allowed, i.e., $2\omega > |E_1|$. We have shown also that the differential cross sections of two-photon free-free transitions are sensible with respect to the helicity of the polarization vectors. These effects are present only if the atomic diagrams (Fig.1c) are included in the calculation.

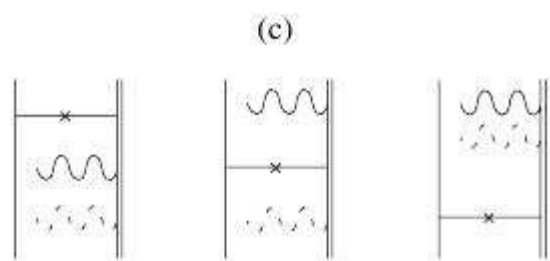
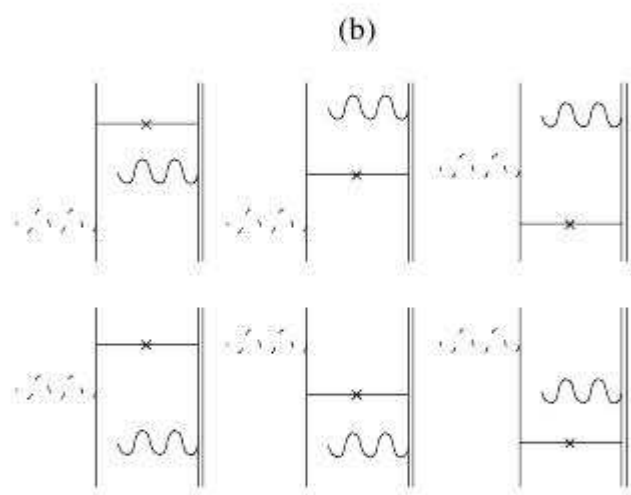
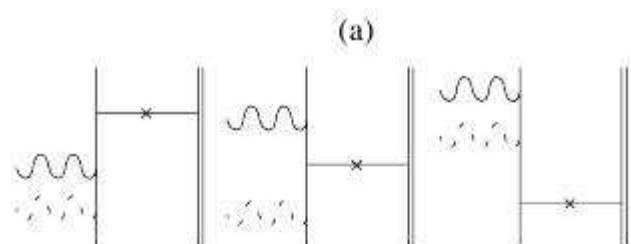
Acknowledgement

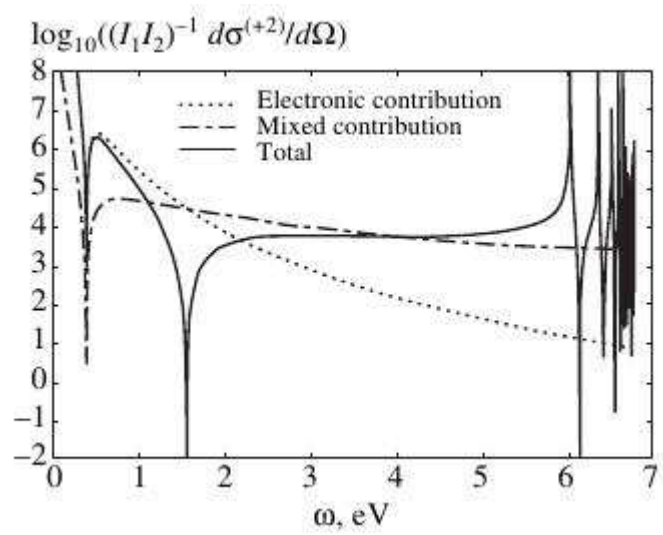
This research is supported in part by the EC PECO contract no ERB CIPD CT940025. Part of the computations were performed in the Computer Center of the Quantum and Statistical Physics Group (Bucharest-Măgurele), supported by SOROS Foundation. One of the authors (A.C.) is indebted to A. Maquet for interesting discussions. A critical reading of the manuscript by V. Florescu is warmly acknowledged.

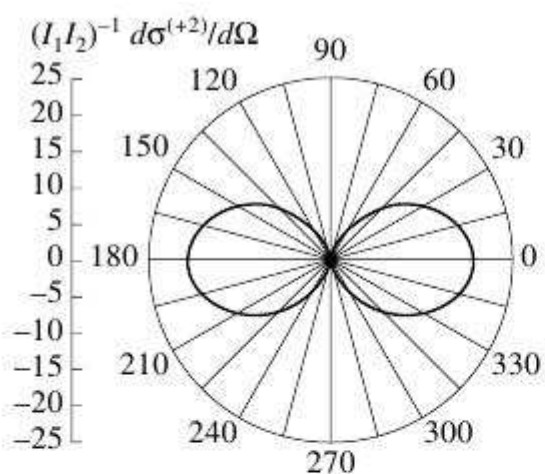
-
- [1] B. Wallbank and J. K. Holmes, J. Phys. B **27**, 1221 (1994), and J. Phys. B **27**, 5405(1994)
- [2] A. Cionga, L. Dimou, and F.H.M. Faisal, J. Phys. B **30**, L361 (1997); see also the references herein
- [3] G. Kracke, J. S. Briggs, A. Dubois, A. Maquet, and V. Vénard, J. Phys. B **27**, 3241 (1994)
- [4] M. Dörr, C. J. Joachain, R. M. Potvliege and S. Vukić, Phys. Rev. A **49**, 4852 (1994)
- [5] F.V. Bunkin and M.V. Fedorov, Zh. Eksp. Teor. Fiz. **49**, 1215 (1965) [Sov. Phys. JETP **22**,884 (1966)]
- [6] V. Florescu and T. Marian, Phys. Rev. A **34**, 4641 (1986)
- [7] A. Cionga and V. Florescu, Phys. Rev. A **45**, 5282 (1992)
- [8] V. Florescu, A. Halasz, and M. Marinescu, Phys. Rev. A **47**, 394 (1993)
- [9] A. Cionga and G. Buică, to be published

Figure captions

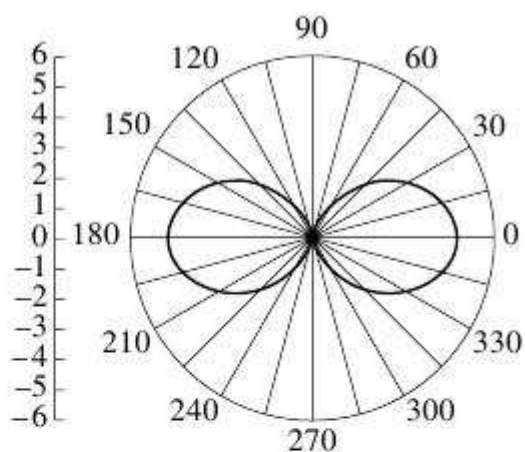
- **Figure 1** Feynman diagrams for two-photon processes in laser-assisted electron-atom scattering. (a) electronic diagrams, (b) mixed diagrams, and (c) atomic diagrams. The projectile is represented by a single line, the bound electron by a double line.
- **Figure 2** The differential cross section for two-photon absorption, normalized with respect to field intensities $I_1 I_2$, as a function of the frequency of the photons. I_1 , I_2 and $d\sigma^{(+2)}/d\Omega$ are in a.u. The energy of the projectile is $E_i = 100$ eV; $\vec{k}_i || Oz$ and the scattering angle is $\theta = 5^\circ$. The polarization vectors are linear: $\vec{\varepsilon}_1 || Oz$ and $\vec{\varepsilon}_2 || Ox$. Solid line represents the differential cross section in Eq.(24), dotted line the electronic contribution and dot-dashed line the mixed contribution.
- **Figure 3** The differential cross section for two-photon absorption, normalized with respect to field intensities $I_1 I_2$, as a function of the azimuthal angle ϕ . I_1 , I_2 and $d\sigma^{(+2)}/d\Omega$ are in a.u. The energy of the projectile is $E_i = 100$ eV, $\vec{k}_i || Oz$ and the scattering angle is $\theta = 20^\circ$. The frequency of the photons is $\omega = 5$ eV, $\vec{\varepsilon}_1 = \vec{e}_z$ and $\vec{\varepsilon}_2 = (\vec{e}_z + i\vec{e}_x)/\sqrt{2}$. The electronic, mixed and atomic contributions are also plotted in the same conditions as the differential cross section.
- **Figure 4** Same as Fig.3, but $\omega = 10$ eV.
- **Figure 5** Same as Fig.3, but $\vec{\varepsilon}_1 \equiv (\vec{e}_z + i\vec{e}_x)/\sqrt{2}$ and $\vec{\varepsilon}_2 \equiv (\vec{e}_y + i\vec{e}_z)/\sqrt{2}$.
- **Figure 6** Same as Fig.5, but $\omega = 10$ eV.



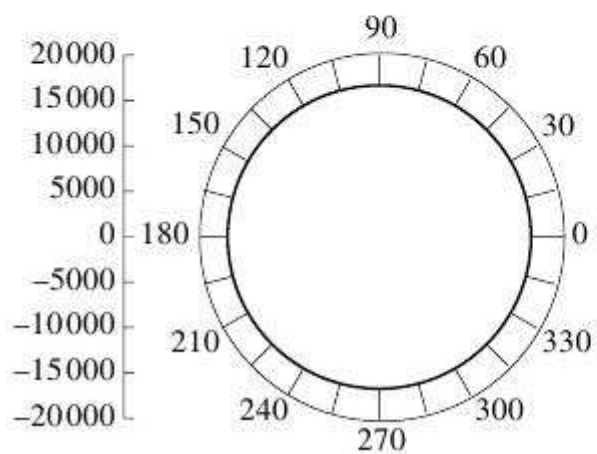




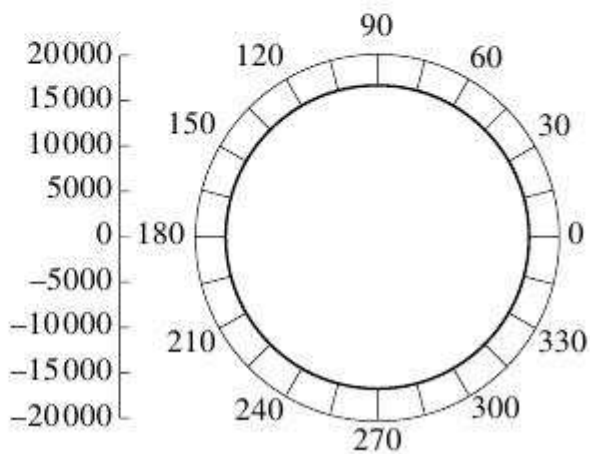
Electronic contribution



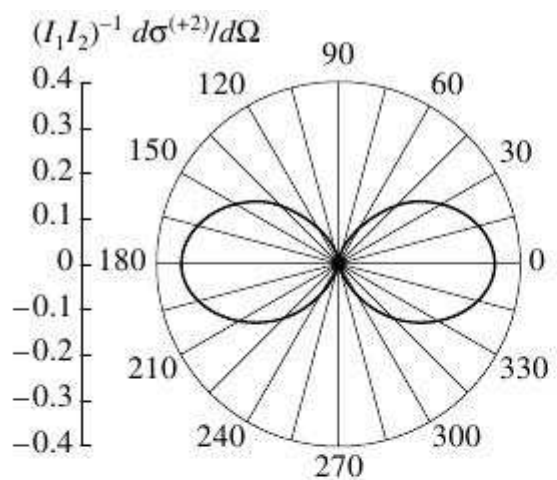
Mixed contribution



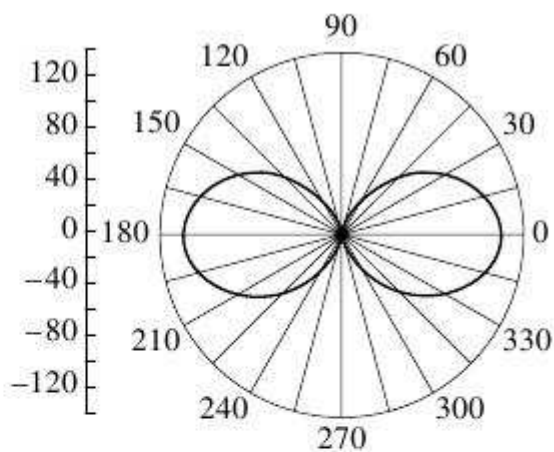
Atomic contribution



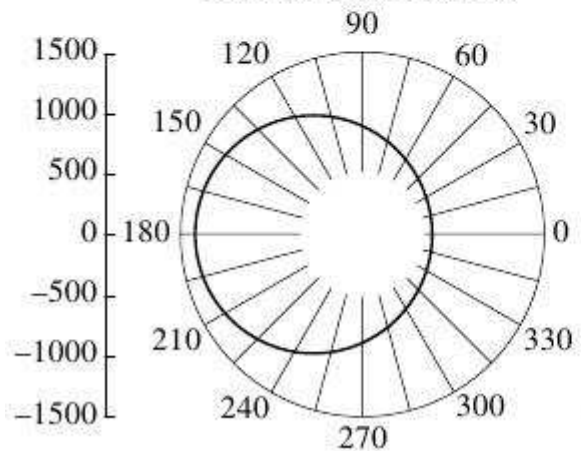
Total



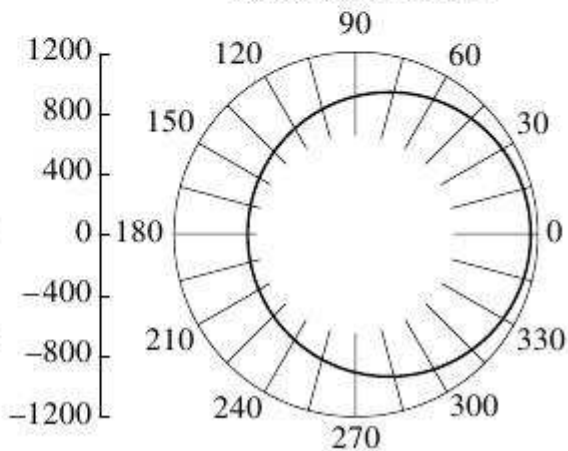
Electronic contribution



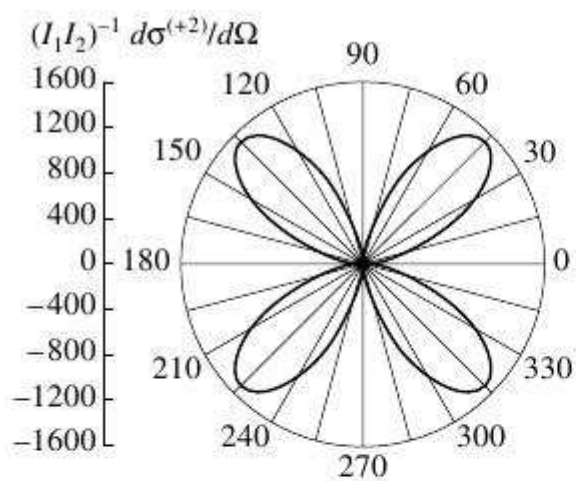
Mixed contribution



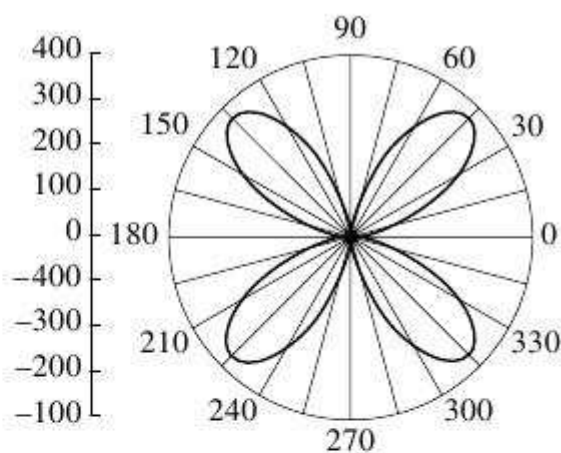
Atomic contribution



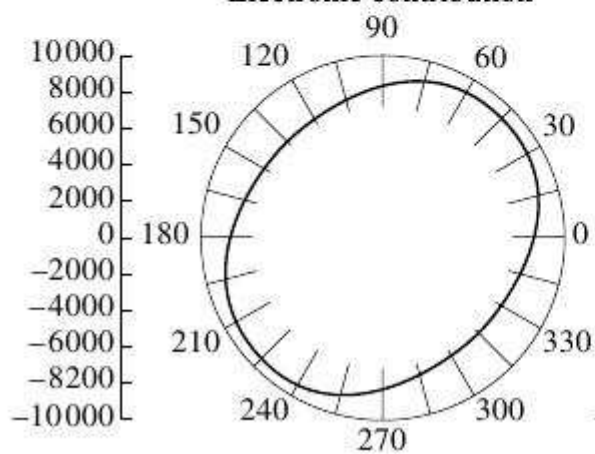
Total



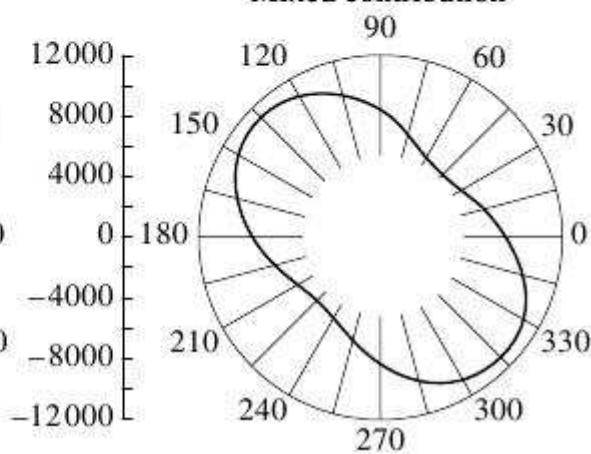
Electronic contribution



Mixed contribution

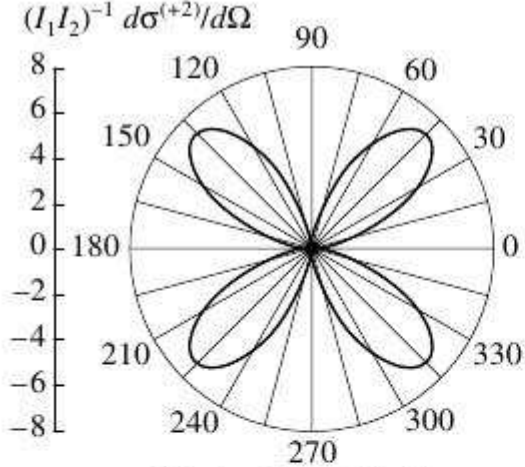


Atomic contribution

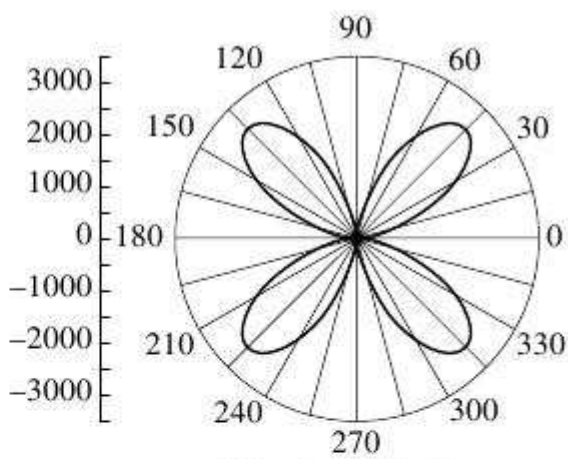


Total

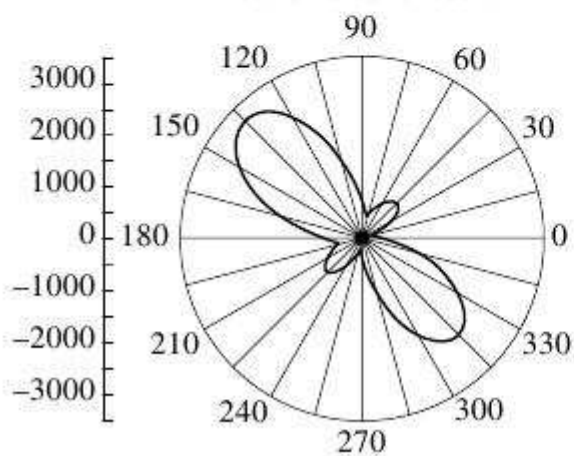
$$(I_1 I_2)^{-1} d\sigma^{(+2)}/d\Omega$$



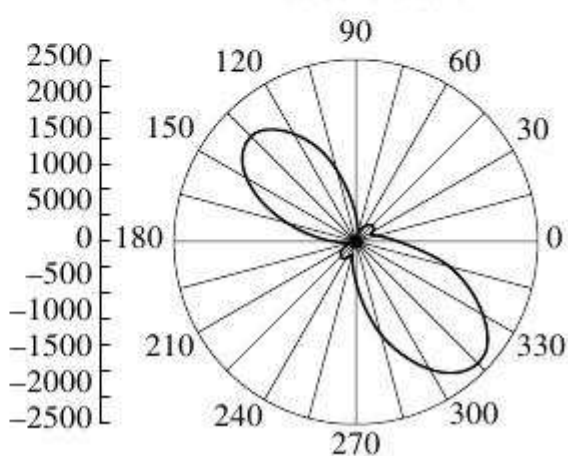
Electronic contribution



Mixed contribution



Atomic contribution



Total